FEMS Microbes, 2025, **6**, xtae034
DOI: 10.1093/femsmc/xtae034
Advance access publication date: 23 December 2024
Research Article – Microbes & Metabolism

Proteomic identification of a *Toxoplasma gondii* sporozoite-specific antigen using HDAC3 inhibitor-treated tachyzoites as surrogate

David Warschkau [1,2], Sandra Klein[1], Ella Schadt[1], Joerg Doellinger[3], Gereon Schares [4], Frank Seeber [1,*]

[1]FG16: Mycotic and Parasitic Agents and Mycobacteria, Robert Koch Institute, 13353 Berlin, Germany
[2]Humboldt-Universität zu Berlin, Department of Biology, 10099 Berlin, Germany
[3]ZBS6: Proteomics and Spectroscopy, Robert Koch Institute, 13353 Berlin, Germany
[4]Friedrich-Loeffler-Institut, Federal Research Institute for Animal Health, Institute of Epidemiology, National Reference Laboratory for Toxoplasmosis, 17493 Greifswald-Insel Riems, Germany
*Corresponding author. FG16: Mycotic and Parasitic Agents and Mycobacteria, Robert Koch Institute, 13353 Berlin, Germany. E-mail: seeberf@rki.de
Editor: [Kathleen Scott]

Abstract

The apicomplexan parasite *Toxoplasma gondii* has a complex life cycle. Access to sexual stages and sporozoite-containing oocysts, essential for studying the parasite's environmental transmission, is limited and requires animal experiments with cats. Thus, alternatives and resource-efficient methods are needed. Several molecular factors and transcriptional switches responsible for differentiation have been identified in recent years. In tachyzoites, drug-induced inhibition of the histone deacetylase HDAC3, or genetic depletion of transcription factors regulating HDAC3, leads to the expression of genes that are specific to sexual stages and oocysts. Here, we applied this concept and showed that the commercially available HDAC3 inhibitor apicidin could be used to identify the hitherto unknown antigen of the sporozoite-specific monoclonal antibody G1/19 in tachyzoites. Using mass spectrometry of immunoprecipitated G1/19 target protein from apicidin-treated cultures, we identified it as SporoSAG. In addition, for the much less abundant sporozoite-specific protein LEA860, apicidin treatment was still sufficient to induce a detectable protein level in immunofluorescence microscopy. We also discuss further applications and the limitations of this approach. This allows to overcome issues with the paucity of material of sexual stages and oocysts from *T. gondii* to some extent without the need for cat-derived material.

Keywords: sexual stages; sporozoites; Apicomplexa; proteomics; late embryogenesis abundant proteins

Introduction

Toxoplasma gondii, the causative agent of toxoplasmosis, has evolved a complex life cycle between multiple host species to ensure optimal spread of the parasite. Environmental transmission occurs through sporozoite-containing oocysts, which are the product of sexual replication restricted to felid hosts (Delgado et al. 2022). An improved understanding of these stages is crucial for advancing the development of vaccines and drugs aimed at preventing and controlling toxoplasmosis.

While tachyzoites can be readily cultured *in vitro*, working on sexual stages and oocysts is difficult since accessibility to enough material for research is limited. Only few labs worldwide can work with infected cats, and those that do face public criticism (Wadman 2019). For this reason, it is important to work resource-saving or find even alternatives for some experimental approaches. We previously reported a method that allows working with very limited amounts of oocysts for high-resolution immunofluorescent assay (IFA) experiments (Fabian et al. 2021).

Recently, it was shown that conditional genetic depletion of tachyzoites of the microrchidia (MORC) protein, a master regulator of downstream Apetala 2 (AP2) transcription factors, resulted in the expression of non-tachyzoite genes (Farhat et al. 2020). Among those were hundreds that are known to be expressed in the sexual stages of the parasite, including oocysts and sporozoites. Notably, a similar phenotype was observed when the compound FR235222 was used. It is a known inhibitor of *T. gondii*'s histone deacetylase 3 (HDAC3) (Bougdour et al. 2009, Sindikubwabo et al. 2017). This suggested the possibility to use drug-treated tachyzoites as a source for transcripts or proteins of oocysts.

We show that apicidin (Darkin-Rattray et al. 1996), an HDAC3 inhibitor with similar structure and properties as FR235222 but commercially available, can be used to identify the target protein of a previously described monoclonal antibody (mAb). This mAb, called G1/19, was shown to stain exclusively sporozoites, but its target protein was unknown (Gondim et al. 2016). Using mass spectrometry of G1/19-immunoprecipitable protein, we identify it as SporoSAG (SRS28; TGME49_258 550). Another oocyst-specific protein could also be detected by immunofluorescence, although it was predicted to be much less abundant. In addition, apicidin treatment allows the cloning of intron-containing genes when sexual stage material is not available but recombinant protein expression is desired and requires spliced mRNA. The general applicability of the approach is discussed.

Received 6 September 2024; **revised** 26 November 2024; **accepted** 19 December 2024

Materials and methods

Cell culture, parasites, and hybridoma production

Human foreskin fibroblasts (HFF; BJ-5ta, ATCC CRL-4001) were grown in DMEM High Glucose (4.5 g/l) with Stable Glutamine (Capricorn Scientific, Cat. No. DMEM-HPSTA) supplemented with 10% fetal bovine serum (FBS), 1×P/S (100 U/ml penicillin and 100 µg/ml streptomycin) at 37°C in 5% CO_2. *Toxoplasma gondii* strains RHΔ*KU80*Δ*HX* and ME49Δ*KU80* tachyzoites were maintained by continuous passage in confluent monolayers of HFF cells in infection medium (DMEM High Glucose (4.5 g/l) with Stable Glutamine, 2% FBS and 1×P/S).

The generation of mAb G1/19 has been previously described (Gondim et al. 2016). Briefly, it derived from the subcutaneous immunization of mice with a suspension containing 100 µg of *T. gondii* oocyst antigen extracted from sporulated oocysts (ME-49 strain; kindly provided by J.P. Dubey, Beltsville, USA) that had previously been treated with sodium hypochlorite.

Infection and apicidin treatment

Toxoplasma gondii-infected host cells were scraped from T75 cell culture flasks, and tachyzoites were released by repeated passes through a 23 G tubing. Cell debris was removed by centrifugation at 100 *g* for 5 min. The supernatant was collected and centrifuged at 300 *g* for 10 min to pellet the tachyzoites. For immunoprecipitation coupled with mass spectrometry (IP-MS), fresh HFF monolayers in four T75 flasks were infected with 2.7×10^7 parasites per flask. For Western blot, T25 flasks were infected with 5.4×10^6 parasites. For IFA, host cells grown on chambered coverslips (8 well ibiTreat µ-Slides, Ibidi) were infected with 7.2×10^4 type II strain parasites or 2.4×10^4 type I strain parasites per well. After 24 h, the medium was changed, and fresh infection medium with 75 nM apicidin (Adipogen) was added. On the same day, another round of infection was performed, which served as the untreated control. After 24 h, samples were processed for IP-MS, Western blot, and immunofluorescence assay (IFA).

Immunoprecipitation and MS sample preparation

The Pierce MS-Compatible Magnetic IP Kit (Protein A/G; Thermo Scientific, Cat. No. 90 409) was used for the immunoprecipitation and MS sample preparation. The kit's lysis buffer was supplemented with protease inhibitor (Roche, cat. no. 4693159001). Apicidin-treated and untreated parasites were released as described above and washed once with phosphate-buffered saline (PBS) and centrifuged at 1200 *g* for 5 min at 4°C. The pellets were resuspended in 1 ml lysis buffer and incubated on ice for 10 min. The samples were sonicated for 10 min and centrifuged at 12 500 *g* for 10 min at 4°C. The supernatants were transferred to new low protein-binding microcentrifuge tubes. The protein concentration was determined by BCA assay (Thermo Scientific, cat. no. 23227). Per IP reaction, 240 µg of total protein was incubated with or without 200 µl of G1/19 hybridoma supernatant overnight at 4°C with mixing to form the immune complex. For immunoprecipitation, the kit manufacturer's protocol was followed, and the modified IP-MS Wash Buffer A with 10 mM $MgCl_2$ was used, as G1/19 is a mouse IgG_1 antibody subtype. The samples were reduced, alkylated, and trypsin-digested according to the manufacturer's protocol.

Liquid chromatography and mass spectrometry

Peptides were analysed on an Evosep One (Evosep, Odense, Denmark) liquid chromatography system coupled online via the CaptiveSpray source to a timsTOF HT mass spectrometer (Bruker Daltonics, Bremen, Germany). A volume of 1 µg of peptides were manually loaded onto Evotips Pure (Evosep) and separated using the 60 samples per day method on the respective performance column (8 cm × 150 µm, 1.9 µm, Evosep). Column temperature was kept at 40°C using a column toaster (Bruker Daltonics), and peptides were ionized using electrospray with a CaptiveSpray emitter (10 µm i.d., Bruker Daltonics) at a capillary voltage of 1400 V. The timsTOF HT was operated in ddaPASEF mode in the *m/z* range of 100–1700 and in the ion mobility (IM) range of 0.65–1.35 Vs/cm^2. Singly charged precursors were filtered out based on their *m/z*-IM position. Precursor signals above 2500 arbitrary units were selected for fragmentation using a target value of 20 000 arbitrary units and an isolation window width of 2 Th below 700 Da and 3 Th above 700 Da. Afterwards, fragmented precursors were dynamically excluded for 0.4 min. The collision energy was decreased as a function of the IM from 59 eV at $1/K_0 = 1.6$ Vs/cm to 20 eV at $1/K_0 = 0.6$ Vs/cm. One cycle consisted of 10 PASEF ramps.

Mass spectrometric data analysis

The LC-IMS-MS/MS data were analysed using FragPipe (version 19.1) (Yu et al. 2020). Spectra were searched using MSFragger against the protein sequences of the human proteome (UP000005640, downloaded 4/28/23, UniProtKB) and the *T. gondii* proteome (UP000001529, downloaded 4/28/23, UniProtKB), with a precursor and fragment mass tolerance of 20 ppm, strict trypsin specificity (KR), and allowing up to two missed cleavage sites. Cysteine carbamidomethylation was set as a fixed modification and methionine oxidation, N-terminal acetylation of proteins were set as variable modifications. Search results were validated using Percolator with MSBooster enabled rescoring and converged to false discovery rates of 1% on all levels. Proteins were quantified using IonQuant with enabled match between run. The statistical analysis of the FragPipe results was done in Perseus (Version 1.6.5.0) (Tyanova et al. 2016). Potential binding partners were identified from the bait samples using FDR-adjusted *P*-values from a *t*-test with a permutation-based FDR of 0.01 and s0 = 1 using the log-2 transformed MaxLFQ intensities. The prey sample group was combined from three control groups (no apicidin, no antibody, and no apicidin and no antibody). The whole analysis was based on using biological triplicates. The mass spectrometry proteomics data have been deposited to the ProteomeXchange Consortium via the PRIDE (Perez-Riverol et al. 2022) partner repository with the dataset identifier PXD055279.

RNA/gDNA extraction and reverse transcription-PCR

Treated tachyzoites were released as described above. After removing the cell debris by centrifugation at 100 *g* for 5 min, the parasites were centrifuged at 1500 *g* for 10 min. The cell pellet of a T25 flask was resuspended in 400 µl TRI Reagent (Zymo, cat. no. R2050-1) and transferred into a 1.5 ml Eppendorf DNA LoBind tube (cat. no. 0 030 108 051). RNA was isolated using the Direct-zol RNA Microprep Kits (Zymo, cat. no. R2062). Genomic DNA contamination was removed by on-column DNase I digestion. RNA was quantified spectrophotometrically at 260/280 nm with the Infinite M200 Pro plate reader (Tecan). RNA was reverse-

transcribed using the High Capacity RNA-to-cDNA Kit (Applied Biosystems) with 500 ng per reaction. For genomic DNA (gDNA) extraction, the cell pellet was processed using the Quick-DNA Microprep Kit (Zymo, cat. no. D3020) following the manufacturer's instructions. Polymerase chain reaction (PCR) was performed with 60 ng template DNA/cDNA using the Q5 High-Fidelity DNA polymerase (NEB) with the recommended reaction setup (including addition of GC enhancer) and thermocycling conditions. Annealing temperature was set to 65°C, and elongation was performed for 1 min per cycle. Cloning primers #1 and #2 with 20 bp overhangs were used (see Table S1). These primers were designed in such a way that sequences encoding the N- and C-terminal topogenic peptidic sequences were removed (see Fig. 2C). Products were visualized by gel electrophoresis on a 2% agarose gel.

Recombinant bacterial expression of SporoSAG

SporoSAG, amplified from cDNA as described above, was inserted by Gibson cloning using the NEBuilder HiFi kit (NEB) into pAvi-MBP-ccdB using primers #3 and #4 for vector amplification, removing the counter-selectable ccdB toxin, as described (López-Ureña et al. 2023). A positive clone was selected (named pAvi-MBP-SporoSAG) and verified by sequencing. It was transformed into the *Escherichia coli* SHuffle strain (NEB) containing plasmid pMJS9 (Klein et al. 2020), which we have shown previously to support the correct folding of the six disulfide bonds of SAG1, another member of the SRS family of *T. gondii* surface proteins. Protein expression and purification followed the protocol for SAG1 (Klein et al. 2020).

Overexpression of LEA860 in tachyzoites

Late Embryogenesis Abundant protein 860 (LEA860) overexpression in tachyzoites was achieved by transfecting RHΔ*KU80*Δ*HX* parasites with a plasmid containing the constitutive tubulin promoter and the full-length untagged coding sequence of LEA860. It was introduced by site-directed mutagenesis with the NEBuilder HiFi DNA Assembly kit. Transfection and selection followed standard procedures (Striepen and Soldati 2007).

Production and purification of sera

Recombinant LEA850 and LEA860 proteins were produced as described previously (Arranz-Solís et al. 2023), and the storage buffer was exchanged to PBS. Antigens were shipped on ice to Preclinics GmbH (Germany) for rabbit immunization. Each animal received four times 150 µg protein in Freund's Adjuvant over a period of 100 days.

Affinity purification of antibodies from rabbit sera was carried out using affinity columns prepared in-house, in which the respective 6His-tagged LEA proteins were irreversibly conjugated to cobalt-based TALON resin by addition of H_2O_2 as described previously (Hale 1995, Bednarek et al. 2003) with some modifications as follows. Briefly, 1.5 ml of TALON resin (Clontech) was washed with buffer A [50 mM Tris–HCl (pH 7.4), 300 mM NaCl] in a microcentrifuge tube after which 750 µl of 10 µM 6His-tagged LEA proteins in buffer A were added and incubated for 30 min at room temperature on a rotating wheel. Then, H_2O_2 was added to a final concentration of 100 mM, and the resin was incubated for 1 h. After several washes with buffer A, 750 µl of serum were added and incubated under rotation for 2 h at 4°C. The resin was transferred to a flow-through column, washed 5 times with buffer A, before bound antibodies were eluted with low pH buffer (0.1 M Glycine-HCl pH 2.5). 1 M Tris–HCl (pH 9) was added for neutralization. Antibodies were finally concentrated, and the buffer was exchanged to PBS (pH 7.4) by centrifugal filtration (30k MWCO, Sartorius Vivaspin 2).

To produce antibodies against TgSAG1, the highly purified recombinant protein (1250 µg; Klein et al. 2020) was used for immunization of an alpaca (Prelinics). It was used unpurified for Western blot and IFA, with no visible unspecific background using appropriate dilutions (Fig. S1).

Western blot analysis

Cells were lysed in RIPA buffer (150 mM NaCl, 50 mM Tris–HCl pH 8.0, 1% IGEPAL CA-630, 0.5% sodium deoxycholate, 0.1% SDS, and protease inhibitor cocktail) and sonicated. Laemmli buffer was added to the samples (final concentrations: 62.5 mM Tris–HCl, 2% SDS, 5% glycerol, 0.1% bromophenol blue). Samples contained no reducing agent and were heated at 95°C for 5 min, then centrifuged, and supernatant was loaded on 12% gels for sodium dodecyl sulfate–polyacrylamide gel electrophoresis (SDS-PAGE). Proteins were transferred to nitrocellulose membranes by wet or semi-dry transfer. Immunostaining was performed with G1/19 mAb hybridoma supernatant 1:10 or anti-His mAb (MAK 1396, Linaris, Germany; 1:1000) in 5% bovine serum albumin in Tris-buffered saline with 0.05% Tween 20 (TBS-T) overnight. The anti-mouse HRP-linked secondary antibody (7076S, Cell Signaling) was used at 1:2000 in TBS-T for 1 h. HRP signal was detected using ECL Plus Western blotting detection reagents on a Vilber fusion FX imaging system.

Immunofluorescence microscopy

After treatment, cells were washed with PBS and fixed (4% paraformaldehyde and 0.05% glutaraldehyde in PBS) for 20 min at room temperature, quenched with 50 mM NH_4Cl in PBS for 15 min, washed with PBS twice, permeabilized (100 mM glycine, 0.25% Triton X-100 in PBS) for 20 min, and blocked with blocking buffer (3% bovine serum albumin in PBS) for 1 h at room temperature. Primary antibodies diluted in blocking buffer were incubated overnight at 4°C. Anti-TgLEA860 rabbit antibody was used at 1:2000, G1/19 mAb hybridoma supernatant (Gondim et al. 2016) was used at 1:10, anti-SAG1 alpaca serum was used at 1:500, and anti-GRA5 mAb 17–113 (Lecordier et al. 1993) (BioVision, Cat# A1299) was used at 1:500. After three washes with PBS containing 0.05% Tween (PBS-T), cells were incubated with secondary antibodies and DAPI in blocking buffer for 2 h at room temperature. Anti-llama Alexa Fluor 488 (Jackson ImmunoResearch, Cat# 128-545-160), anti-rabbit Alexa Fluor 568 (Invitrogen, Cat# A-10042), and anti-mouse Cy5 (Jackson ImmunoResearch, Cat# 115-175-146) were used 1:250. Cells were then washed three times with PBS-T, once with PBS. Chambered slides were mounted with Ibidi mounting medium, and coverslips were mounted onto a glass slide with Fluoromount G. Slides were imaged using a Zeiss LSM780 or Leica Stellaris 8 confocal laser scanning microscope. Images were processed with FIJI 2.3.0 and assembled with Affinity Designer 1.9.2.

Bioinformatic analyses and software used

MarvinSketch (ChemAxon) was used for chemical drawings of structures taken from PubChem. GPI anchor cleavage predictions were done with NetGPI-1.1 and PredGPI, respectively (Pierleoni et al. 2008, Gíslason et al. 2021); SignalP 6.0 was used for signal peptide cleavage prediction (Teufel et al. 2022). Post-translational modification site prediction for glycosylation was performed online with NetOGlyc-4.0 (Steentoft et al. 2013) and MusiteDeep

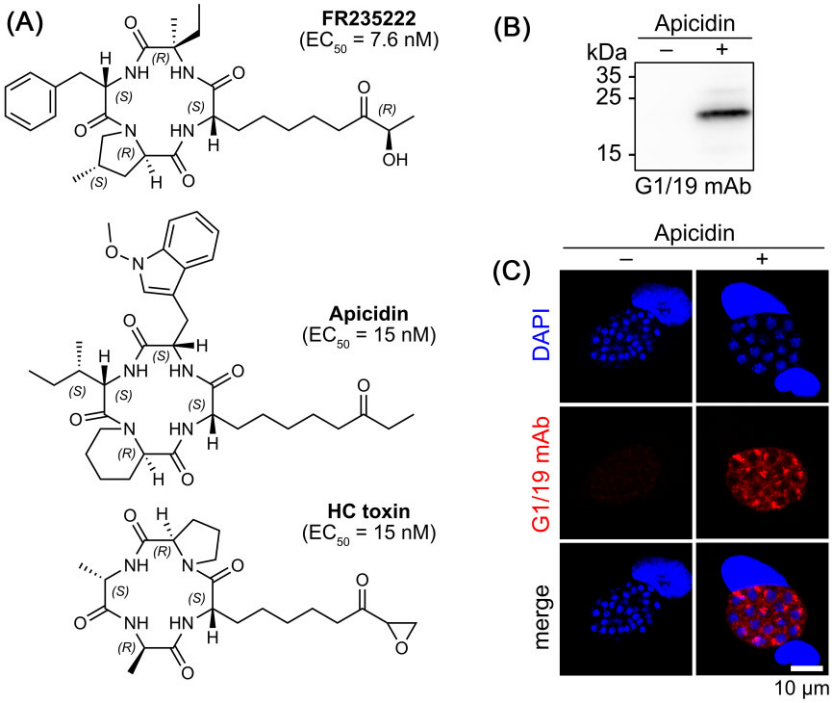

Figure 1. G1/19 antigen is expressed in tachyzoites upon apicidin treatment. (A) Chemical structures of the cyclic tetrapeptides FR235222, apicidin and HC toxin. EC50 values are from Darkin-Rattray et al. (1996) and Bougdour et al. (2009). (B) Western blot analysis of cell lysates under non-reducing conditions with G1/19 mAb. Intracellular ME49Δ*ku80* tachyzoites were treated with 75 nM apicidin for 24 h or left untreated. (C) Immunofluorescence microscopic images of tachyzoites stained with G1/19 mAb. Nuclei were stained with DAPI.

(Wang et al. 2020). Sequences, proteomic, and transcriptomic data were downloaded from ToxoDB (https://toxodb.org/) (Harb et al. 2020). Multiple sequence alignment was visualized with JalView 2 (Waterhouse et al. 2009) and manually finished with Affinity Designer 1.9.

AlphaFold 2 prediction of *Hammondia hammondi* SporoSAG (HHA_258 550) was performed using ColabFold v1.5.3 (https://github.com/sokrypton/ColabFold) using default settings (Mirdita et al. 2022). For structure display and comparison (AF-A0A125YLQ9-F1-model_v4 from ToxoDB; 2wnk from PDBe (https://www.ebi.ac.uk/pdbe/) and ColabFold-predicted Hh-SporoSAG), ChimeraX 1.6.1 and the built-in Matchmaker superposition tool were used (Meng et al. 2023).

Comparison of FR235222-regulated and stage-specific genes was performed using existing RNA-seq datasets of previous studies (Ramakrishnan et al. 2019, Farhat et al. 2020) and obtained from ToxoDB. Stage-specific expression was determined by the fold change and absolute TPM difference with reference to the expression level at the tachyzoite stage. Transcripts were deemed enteroepithelial stage (EES)-specific when the maximum fold change of EES 1 to EES 5 was > 8 and the absolute TPM difference was >10. Oocyst-specific transcripts were classified accordingly using the maximum expression of unsporulated, sporulating, and sporulated oocysts. FR235222-regulated genes were determined with the same threshold values in comparison to untreated parasites (Table S1). Sporozoite data were taken from Kidaka et al. (2022).

Proteomic datasets from oocysts were taken from Possenti et al. (2010), Fritz et al. (2012), Zhou et al. (2016, 2017), and ToxoDB (oocyst proteome M4 from J. Wastling) and combined into a set of 3888 unique sequences (Table S1). The proteins from FR235222-treated PRU strain are from Farhat et al. (2020). Data were visualized using the R package 'ggpubr'.

Results

Apicidin treatment enriches for the G1/19 target protein in tachyzoites

We reasoned that commercially available histone deacetylase inhibitors, such as HC toxin or the more cost-effective apicidin, both of which are structurally similar to FR235222 (Fig. 1A) and target TgHDAC3 in a comparable manner (Bougdour et al. 2009, Sindikubwabo et al. 2017), could be used to induce the expression of sporozoite-specific proteins in tachyzoites in amounts to be detected by proteomics. Using apicidin, we first tested whether the target protein of mAb G1/19 would be upregulated. On a Western blot of proteins of tachyzoites of strain ME49Δku80, a strong band was observed at ~23 kDa and a faint signal at around 30 kDa upon apicidin treatment (Fig. 1B). No reactivity was observed in the untreated control. Notably, no signal was observed under reducing conditions (50 mM TCEP), suggesting that disrupting disulfide bonds affects the G1/19 epitope (Fig. S2). Treated tachyzoites were also analysed by IFA. A signal of bound antibody was observed within the parasites and the parasitophorous vacuole only after treatment with apicidin (Fig. 1C). It substantially impacted the morphology of the parasites in a dose-dependent fashion (Fig. S3A). Treated tachyzoites appeared swollen and more globular (as described previously for FR235222-treated tachyzoites; Bougdour et al. 2009), and individual parasites were not easily distinguishable within the parasitophorous vacuole, an observation we made when staining for SAG1, the main surface antigen of tachyzoites (Fig. S3B). This limits drawing conclusions about the physiological localization of the G1/19 antigen.

Taken together, these results provided strong evidence that apicidin treatment of tachyzoites leads to the expression of a 23 kDa protein to which mAb G1/19 binds, corroborating previous results with the conditional MORC-KD strain (Farhat et al. 2020).

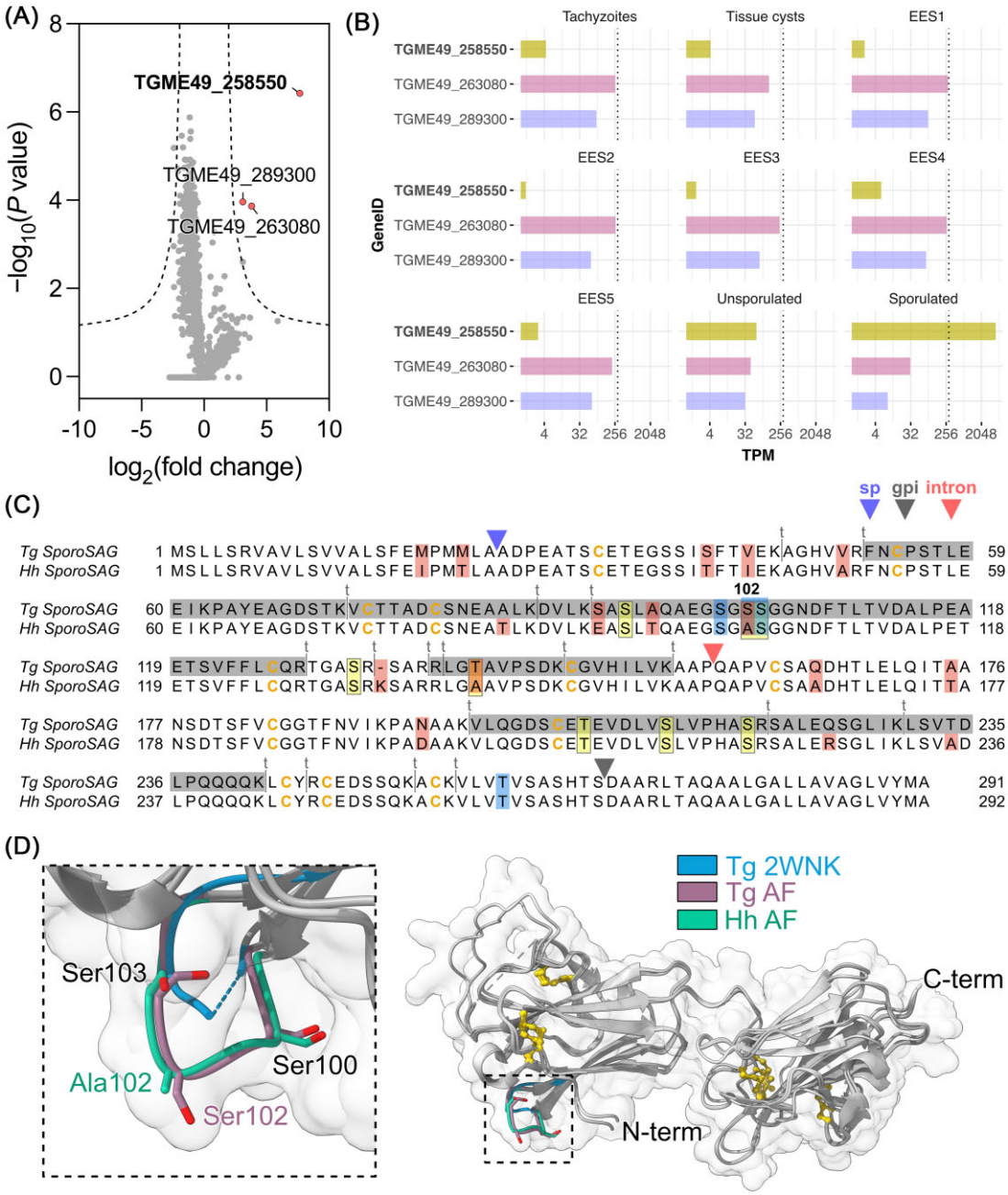

Figure 2. SporoSAG is the antigen recognized by mAb G1/19, as revealed by IP-MS and sequence features. (A) Volcano plot of MS analysis showing proteins enriched by immunoprecipitation with G1/19 mAb. Fold change represents IP with G1/19 mAb versus controls. Highlighted are significantly enriched proteins based on a *t*-test (false discovery rate < 0.01, s0 = 1; threshold is indicated by dashed lines). (B) Expression of the three candidate G1/19 antigens *in vivo*. Raw data are from Ramakrishnan et al. (2019) via ToxoDB, showing expression levels derived from RNAseq experiments as TPM (transcripts per million). EES1-5 denote the enteroepithelial stages; sporulated or unsporulated are oocysts of the respective stage. The dashed line is at 300 TPM. (C) Sequence comparison of *T. gondii* SporoSAG with the homolog from *H. hammondi* together with some sequence features. Cysteines involved in disulfide bonds are in dark yellow. Cleavage site predictions for signal peptide (sp) and GPI anchor addition (gpi) as well as the insertion point of the single intron are indicated by arrowheads. The peptides identified by MS are shaded in gray, with the trypsin cleavage sites (t) indicated. Red-shaded residues differ between both proteins; those in blue and yellow are potential glycosylation sites predicted by NetOGlyc-4.0 or MusiteDeep, respectively. Residues 102 and 103 of the *T. gondii* sequence were predicted by both algorithms. (D) Superposition of experimentally and predicted structures of SporoSAG. The 'glycosylation loop' in modeled *T. gondii* SporoSAG (Tg AF, purple) contains the indicated three serines predicted to be glycosylation sites. The respective part in the experimental structure (Tg 2WNK, blue) is missing, reflected by the dotted line. The loop of the AF2 model of *H. hammondi* SporoSAG (Hh AF) is shown in green. Cysteines are drawn as ball-and-stick in yellow. Protein surfaces are shown.

The target of mAb G1/19 is a known protein—SporoSAG

Since the G1/19 antigen was substantially enriched in tachyzoites upon apicidin treatment, we wanted to identify the antigen by a proteomics approach using immunoprecipitation followed by mass spectrometry (IP-MS). To this end, the lysate of treated tachyzoites was incubated with G1/19 hybridoma supernatant. The formed immune complex was then pulled down with Protein A/G beads. The identities of the immunoprecipitated proteins were then determined by mass spectrometry

(Fig. 2A). Three proteins were significantly enriched (false discovery rate < 0.01 by a minimum two-fold enrichment) compared to controls: TGME49_258 550 (SAG-related sequence SRS28, also known as SporoSAG; predicted MW 30 kDa); TGME49_263 080 (ATP synthase-associated protein; 14.4 kDa); and TGME49_289 300 (methionyl-tRNA synthetase; 106 kDa).

We analysed the expression levels of the three proteins *in silico* using full life-cycle transcriptome data of *T. gondii* (Ramakrishnan et al. 2019) (Fig. 2B). This indicated that SporoSAG is highly expressed exclusively in sporulated oocysts, whereas the other two proteins are expressed in all stages and are not specifically upregulated in sporulated oocysts. Likewise, a similar analysis with the published transcriptional data of MORC-KD and FR235222-treated PRU strain, respectively, shows a similar response upon MORC inhibition and shows expression of LEA850 and LEA860, previously reported to be highly oocyst-specific (Arranz-Solís et al. 2023) (Fig. S4A).

Thus, SporoSAG's sporozoite-specific expression described previously (Radke et al. 2004) made it the most likely antigen recognized by mAb G1/19. The theoretical molecular weight of SporoSAG of 30 kDa is higher than the observed size in SDS-PAGE (Fig. 1B) but can be explained by its known structural features (Fig. 2C, D; see also the 'Discussion' section). The protein is suspected to be GPI-anchored, thus requiring N- and C-terminal processing, which could reduce its size by 5 kDa.

Apicidin induces SporoSAG gene expression in tachyzoites

To validate SporoSAG as the antigen of mAb G1/19, we first confirmed its apicidin-dependent gene expression by reverse transcription (RT)-PCR with SporoSAG-specific primers. As expected, an amplicon was only observed after apicidin treatment (Fig. 3A). A control with extracted genomic DNA showed a larger band (775 bp) corresponding to the amplicon including the single intron.

Recombinant SporoSAG is recognized by mAb G1/19

As a final test for mAb G1/19's specificity, we tested by Western blot whether recombinant SporoSAG was recognized by the antibody. SporoSAG's three-dimensional structure has been determined previously and was shown to possess six disulfide bonds important for proper folding (Crawford et al. 2010) (Fig. 2D). We therefore used our previously described *Escherichia coli* expression system that allowed the production of correctly folded SAG1, the major tachyzoite surface antigen of *T. gondii*, as a fusion with maltose-binding protein from *E. coli* (Fig. 3B) (Klein et al. 2020), which served as a negative control protein. The expression product of 70 kDa was recognized by mAb G1/19 (Fig. 3C), although a strong signal required much longer exposure of the Western blot compared to the anti-6His tag monoclonal antibody (see also the 'Discussion' section). The G1/19 antibody did not bind to MBP-SAG1. This proves that SporoSAG is the target protein of mAb G1/19.

LEA proteins are also induced by apicidin

SporoSAG is amongst the most upregulated genes in FR235222-treated tachyzoites on both the transcript and protein levels (Fig. S4A and B), explaining the relative ease to detecting it by IFA and Western blot. A gene with a similar high expression upon apicidin treatment is TGME49_276850. It codes for LEA850, one of four LEA proteins previously identified as being oocyst-specific and presumably being involved in resilience of oocysts to environmental stresses (Arranz-Solís et al. 2023). We were therefore interested in whether a polyclonal rabbit serum generated against purified recombinant LEA850 (Arranz-Solís et al. 2023) would recognize the protein in apicidin-treated tachyzoites by IFA. Although this serum reacted with the antigen used for immunization, it also showed cross-reactivity with the other 6His-tagged LEA proteins (data not shown) and was not further evaluated.

However, the specificity of a serum raised against recombinant LEA860 (encoded by TGME49_276 860) was given once it had been affinity-purified. Surprisingly, although LEA860 protein was not reported in the FR235222-treated proteomics dataset of Farhat et al. and LEA860 gene transcription was much less induced upon drug treatment compared to LEA850 (Fig. S4A and B), an antibody signal exclusively in apicidin-treated tachyzoites was observed (Fig. 4, parental strain). Again, strong morphological changes of treated parasites were obvious, but co-staining with an antibody against GRA5, known to decorate the parasitophorous vacuolar membrane (PVM; Lecordier et al. 1993), outlined the vacuole in apicidin-treated cells. In co-staining, no strong co-localization of GRA5 and LEA860 could be observed, although this might have been expected, since the LEA860 protein sequence contains a predicted signal peptide (Arranz-Solís et al. 2023) and could thus be localized in the vacuole or close to the PVM.

Constitutive expression of LEA860 in tachyzoites leads to its PV localization

Another mAb against SporoSAG (TMS4) has been described previously (Radke et al. 2004) and was used to demonstrate that overexpression of SporoSAG in tachyzoites, using a strong constitutive promoter, resulted in its localization at the parasite membrane, similar to sporozoites. We used a similar approach to verify whether LEA860's predicted signal peptide results in protein secretion and whether there are differences between plus/minus apicidin treatment.

Indeed, LEA860 secretion into the lumen of the parasitophorous vacuole (PV) was observed when its overexpression was under the control of the constitutive tubulin promoter in tachyzoites. The protein accumulated in the PV of intracellular tachyzoites, but a signal at the PVM, as seen with GRA5 co-staining, could not be observed consistently (Fig. 4; Fig. S5). This seems to change upon apicidin treatment, although again the gross morphological changes make it difficult to draw firm conclusions. Taken together, this experiment shows evidence for a functional signal peptide of LEA860 and verifies the serum's specificity for it.

Discussion

We describe the application of a previously reported finding, namely the induction of oocyst stage-specific proteins by treating tachyzoites with HDAC3 inhibitors (Farhat et al. 2020), to identify the hitherto unknown target of an mAb known to be specific for sporozoites (G1/19; Gondim et al. 2016). Using as inhibitor apicidin instead of FR235222 (a drug that is not commercially available), we were able to immunoprecipitate with G1/19 sufficient protein to identify it as SporoSAG by proteomic analysis. This antibody had been used previously for IFA in genetically depleted MORC parasites in which it showed a pattern of reactivity similar to our results (Farhat et al. 2020) (Fig. 1C). Gross morphological changes upon FR235222 treatment, such as vacuolization and lack of

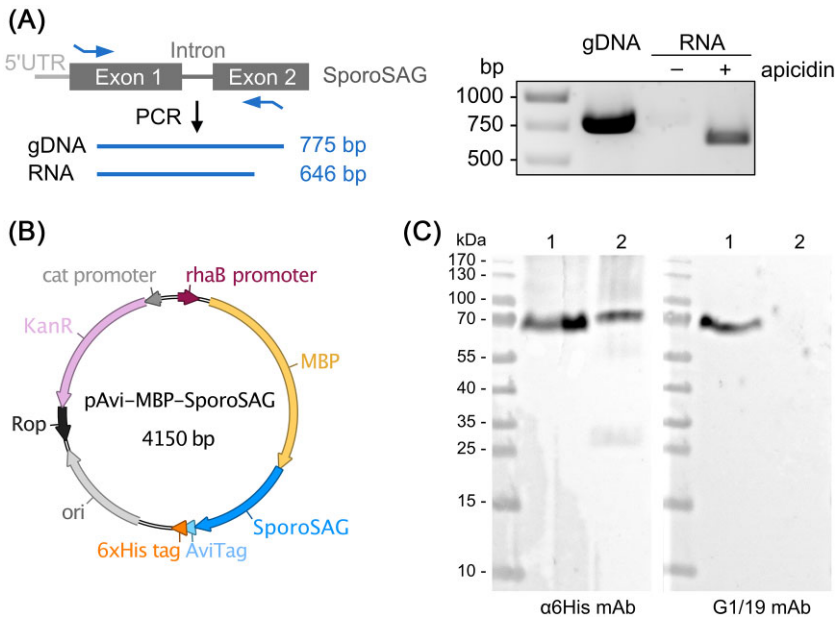

Figure 3. cDNA-derived cloning and recombinant expression of SporoSAG. (A) Schematic drawing of the SporoSAG gene with its intron and two exons (left). The intron is removed in mature messenger RNA. PCR with SporoSAG-specific primers produces a longer intron-containing amplicon when genomic DNA (gDNA) template is used and a shorter intron-free amplicon when RNA template is used. Agarose gel of the PCR products is shown (right). *Toxoplasma gondii* gDNA and RNA extracted from parasites with apicidin treatment (+) or without (–) was used. bp, base pair. UTR, untranslated region. (B) Plasmid map of the construct used to express C-terminally tagged MBP-SporoSAG fusion protein. Expression is controlled by a rhamnose-inducible promoter (rhaB). The MPB-SporoSAG fusion protein has a biotinylation tag (AviTag) in addition to the 6xHis tag. (C) Western blot of purified MBP-SporoSAG (lane 1) probed with anti-6His mAb (left) and mAb G1/19 (right). Lane 2 shows purified MBP-SAG1 as a control. Note that exposure time of the left blot was 1 min compared to 5 min for the one incubated with mAb G1/19 to result in a similar signal strength.

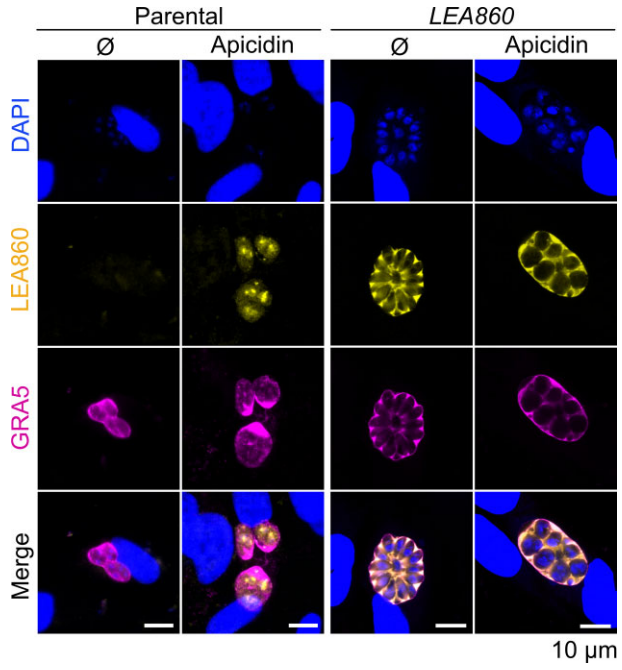

Figure 4. Apicidin treatment induces the expression of the sporozoite protein LEA860. Intracellular tachyzoites of the parental RHΔ*ku80*Δ*hxgprt* or LEA860 overexpression strain were either untreated **(**Ø) or treated with 75 nM apicidin for 24 h and then fixed. Samples were stained with antibodies against LEA860 or GRA5 and DAPI to stain DNA for subsequent confocal immunofluorescence microscopy.

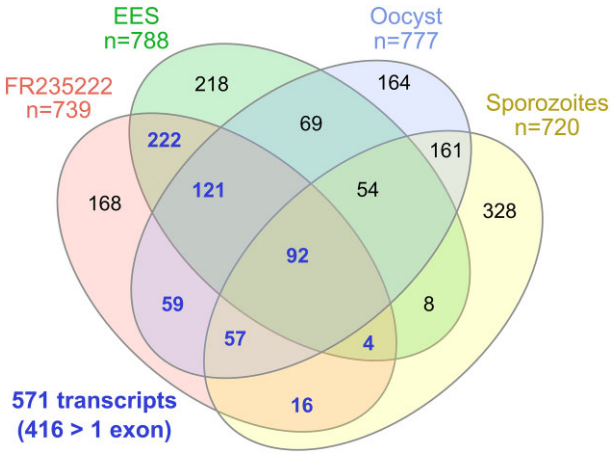

Figure 5. Candidate genes for similar studies. Comparison of genes upregulated in tachyzoites by FR235222 and genes specifically expressed in enteroepithelial stages (EES), oocysts, and sporozoites (see Table S1 for details). Analysis is based on available RNA-seq data (see the 'Methods' section).

daughter cells together with the appearance of aberrant progeny have been reported previously (Bougdour et al. 2009). They thus hamper localization studies, as shown here for SporoSAG and LEA860 after apicidin treatment.

Our proteomics approach was shown for a single protein, but it can be applied to more targets (Fig. 5). Among the 571 genes that show upregulated RNA expression in FR235222-treated tachyzoites and are specifically expressed in the EES, oocyst, or sporozoite stages, 97 showed significant enrichment at the protein level (Farhat et al. 2020).

Another application of apicidin-treated tachyzoites is for RT-qPCR primer validation of genes from sexual stages. Primers spanning an exon-exon junction can greatly enhance specificity (Apte

and Daniel 2009), and 416 *T. gondii* genes in Fig. 5 (73%) have introns (Table S1). However, in the light of reported intron retention in *T. gondii* (Lunghi et al. 2016, Lee et al. 2021), mRNA is required to fully validate the primers to perform as expected. In this respect, drug treatment of tachyzoites is a simple solution for obtaining mRNA of apicidin-responsive genes. Such mRNA from intron-containing genes is also useful when coding sequence is required for recombinant protein expression on a larger scale, e.g. for identification of stage-specific serological markers (López-Ureña et al. 2023).

Apicidin treatment also leads to the expression of bradyzoite genes (Boyle et al. 2006, Maubon et al. 2010, Farhat et al. 2020, Sanchez et al. 2023), and thus the approach could in principle also be applied to this stage. However, there exist protocols to generate bradyzoites *in vitro* in large amounts without drug treatment and resembling the *in vivo* stage (Cerutti et al. 2020, Warschkau and Seeber 2023, Maus et al. 2024).

It was previously reported that mAb G1/19 did not react with *H. hammondi* sporozoites (Gondim et al. 2016). Now that we know the target of this mAb, this is surprising, given that the homologous sequence from this parasite is 94.5% identical to the *T. gondii* sequence (Fig. 2C). Interestingly, comparison of the known *T. gondii* 3D structure (PDB 2WNK) with the two AlphaFold2-predicted structures from *T. gondii* and *H. hammondi* provides a possible explanation for this finding. A possible glycosylation site (predicted by two algorithms; see the 'Materials and methods' section) is in a surface loop predicted by AlphaFold2 but curiously missing in the experimentally determined structure (see Fig. 2D). Notably, one of the two serines potentially being glycosylated, Ser102, is an alanine in *H. hammondi*. We speculate that the epitope of mAb G1/19 is partially dependent on the glycosylation at this loop, which would be missing in *H. hammondi*. It could also explain why mAb G1/19 is only weakly reacting with recSporoSAG since glycosylation is not performed in *E. coli*. In Western blot analysis with G1/19 and oocyst antigen, the observed band of ~30 kDa might also indicate glycosylation (Gondim et al. 2016). Radke et al. reported that TSM4, the other mAb against SporoSAG, strongly reacted with a smear at 25 kDa of oocyst material by Western blots (Radke et al. 2004). The authors attributed this to 'incomplete preservation of intrachain disulphides', but in light of this discussion, it could also be due to glycosylation or a combination of both. Future studies with native and recombinant proteins from sporozoites from *H. hammondi* and *T. gondii* and detailed proteomic analyses will be required to solve this question.

The size of SporoSAG, as seen in Fig. 1B, is still smaller than the 25 kDa expected from the processed protein sequence. This could be due to a GPI anchor, the presence of which could result in a shift towards a small but observable lower molecular size in SDS-PAGE, as has been shown previously for the related SAG1 protein (Seeber et al. 1998). However, whether this size difference is an indication for GPI anchor addition still working under apicidin treatment requires further experiments. At least transcription of the six genes described by Gas-Pascual et al. (2019) as being involved in GIPL and GPI-anchor biosynthesis is not affected in MORC-inhibited cells (data not shown).

In conclusion, the paucity of material of sexual stages and oocysts from *T. gondii* can be overcome to some extent by induction of these genes by treatment of tachyzoites with the HDAC3 inhibitor apicidin. While limited to a few experimental questions like antigen identification by proteomics and IFA or PCR primer verification and cloning of cDNA of intron-containing stage-specific genes, it should encourage further studies on these important parasite stages.

Acknowledgements

We thank Benedikt Fabian for initial help with LEA antibody generation, Andrea Bärwald for technical expertise, Dominique Soldati for parasite strains, and Toni Aebischer for comments on the manuscript. We acknowledge the important role of ToxoDB for making available all the data we used in the manuscript. D.W. is a member of the Research Training Group 2046 'Parasite Infections: From Experimental Models to Natural Systems' funded by the Deutsche Forschungsgemeinschaft (DFG), project no. 251133687/GRK 2046. F.S. and G.S. are members of TOXOSOURCES (supported by funding from the European Union's Horizon 2020 Research and Innovation program under grant agreement number: 773830: One Health European Joint Program). S.K., J.D., and F.S. are supported by the Robert Koch-Institut.

Supplementary data

Supplementary data is available at *FEMSMC Journal* online.

Conflict of interest: None declared.

References

Apte A, Daniel S. PCR primer design. *Cold Spring Harb Protoc* 2009;**2009**:pdb.ip65.

Arranz-Solís D, Warschkau D, Fabian BT *et al.* Late embryogenesis abundant proteins contribute to the resistance of *Toxoplasma gondii* oocysts against environmental stresses. *mBio* 2023;**14**:e0286822.

Bednarek A, Wiek S, Lingelbach K *et al. Toxoplasma gondii*: analysis of the active site insertion of its ferredoxin-NADP(+)-reductase by peptide-specific antibodies and homology-based modeling. *Exp Parasitol* 2003;**103**:68–77.

Bougdour A, Maubon D, Baldacci P *et al.* Drug inhibition of HDAC3 and epigenetic control of differentiation in Apicomplexa parasites. *J Exp Med* 2009;**206**:953–66.

Boyle JP, Saeij JP, Cleary MD *et al.* Analysis of gene expression during development: lessons from the Apicomplexa. *Microbes Infect* 2006;**8**:1623–30.

Cerutti A, Blanchard N, Besteiro S. The bradyzoite: a key developmental stage for the persistence and pathogenesis of toxoplasmosis. *Pathogens* 2020;**9**:234.

Crawford J, Lamb E, Wasmuth J *et al.* Structural and functional characterization of SporoSAG: a SAG2-related surface antigen from *Toxoplasma gondii*. *J Biol Chem* 2010;**285**:12063–70.

Darkin-Rattray SJ, Gurnett AM, Myers RW *et al.* Apicidin: a novel antiprotozoal agent that inhibits parasite histone deacetylase. *Proc Natl Acad Sci USA* 1996;**93**:13143–7.

Delgado ILS, Zúquete S, Santos D *et al.* The apicomplexan parasite *Toxoplasma gondii*. *Encyclopedia* 2022;**2**:189–211.

Fabian BT, Lepenies B, Schares G *et al.* Expanding the known repertoire of C-type lectin receptors binding to *Toxoplasma gondii* oocysts using a modified high-resolution immunofluorescence assay. *mSphere* 2021;**6**:e01341–20.

Farhat DC, Swale C, Dard C *et al.* A MORC-driven transcriptional switch controls *Toxoplasma* developmental trajectories and sexual commitment. *Nat Microbiol* 2020;**5**:570–83.

Fritz HM, Bowyer PW, Bogyo M *et al.* Proteomic analysis of fractionated *Toxoplasma* oocysts reveals clues to their environmental resistance. *PLoS One* 2012;**7**:e29955.

Gas-Pascual E, Ichikawa HT, Sheikh MO *et al.* CRISPR/Cas9 and glycomics tools for *Toxoplasma* glycobiology. *J Biol Chem* 2019;**294**:1104–25.

Gíslason MH, Nielsen H, Almagro Armenteros JJ *et al.* Prediction of GPI-anchored proteins with pointer neural networks. *Curr Res Biotechnol* 2021;**3**:6–13.

Gondim LF, Wolf A, Vrhovec MG *et al.* Characterization of an IgG monoclonal antibody targeted to both tissue cyst and sporocyst walls of *Toxoplasma gondii*. *Exp Parasitol* 2016;**163**:46–56.

Hale JE. Irreversible, oriented immobilization of antibodies to cobalt-iminodiacetate resin for use as immunoaffinity media. *Anal Biochem* 1995;**231**:46–9.

Harb OS, Kissinger JC, Roos DS. Chapter 23–ToxoDB: the functional genomic resource for *Toxoplasma* and related organisms. In: Weiss LM, Kim K (eds), *Toxoplasma gondii*(3rd edn), London, Academic Press, 2020, 1021–41.

Kidaka T, Sugi T, Hayashida K *et al.* TSS-seq of *Toxoplasma gondii* sporozoites revealed a novel motif in stage-specific promoters. *Infect Genet Evol* 2022;**98**:105213.

Klein S, Stern D, Seeber F. Expression of *in vivo* biotinylated recombinant antigens SAG1 and SAG2A from *Toxoplasma gondii* for improved seroepidemiological bead-based multiplex assays. *BMC Biotechnol* 2020;**20**:53.

Lecordier L, Mercier C, Torpier G *et al.* Molecular structure of a *Toxoplasma gondii* dense granule antigen (GRA 5) associated with the parasitophorous vacuole membrane. *Mol Biochem Parasitol* 1993;**59**:143–53.

Lee VV, Judd LM, Jex AR *et al.* Direct nanopore sequencing of mRNA reveals landscape of transcript isoforms in apicomplexan parasites. *Msystems* 2021;**6**:e01081–20.

López-Ureña N-M, Calero-Bernal R, Koudela B *et al.* Limited value of current and new in silico predicted oocyst-specific proteins of *Toxoplasma gondii* for source-attributing serology. *Front Parasitol* 2023;**2**:1292322.

Lunghi M, Spano F, Magini A *et al.* Alternative splicing mechanisms orchestrating post-transcriptional gene expression: intron retention and the intron-rich genome of apicomplexan parasites. *Curr Genet* 2016;**62**:31–8.

Maubon D, Bougdour A, Wong YS *et al.* Activity of the histone deacetylase inhibitor FR235222 on *Toxoplasma gondii*: inhibition of stage conversion of the parasite Cyst form and study of new derivative compounds. *Antimicrob Agents Chemother* 2010;**54**:4843–50.

Maus D, Curtis B, Warschkau D *et al.* Generation of mature *Toxoplasma gondii* bradyzoites in human immortalized myogenic KD3 cells. *Bio Protoc* 2024;**14**:e4916.

Meng EC, Goddard TD, Pettersen EF *et al.* UCSF ChimeraX: tools for structure building and analysis. *Protein Sci* 2023;**32**:e4792.

Mirdita M, Schütze K, Moriwaki Y *et al.* ColabFold: making protein folding accessible to all. *Nat Methods* 2022;**19**:679–82.

Perez-Riverol Y, Bai J, Bandla C *et al.* The PRIDE database resources in 2022: a hub for mass spectrometry-based proteomics evidences. *Nucleic Acids Res* 2022;**50**:D543–D552.

Pierleoni A, Martelli PL, Casadio R. PredGPI: a GPI-anchor predictor. *BMC Bioinf* 2008;**9**:392.

Possenti A, Cherchi S, Bertuccini L *et al.* Molecular characterisation of a novel family of cysteine-rich proteins of *Toxoplasma gondii* and ultrastructural evidence of oocyst wall localisation. *Int J Parasitol* 2010;**40**:1639–49.

Radke JR, Gubbels MJ, Jerome ME *et al.* Identification of a sporozoite-specific member of the *Toxoplasma* SAG superfamily via genetic complementation. *Mol Microbiol* 2004;**52**:93–105.

Ramakrishnan C, Maier S, Walker RA *et al.* An experimental genetically attenuated live vaccine to prevent transmission of *Toxoplasma gondii* by cats. *Sci Rep* 2019;**9**:1474.

Sanchez SG, Bassot E, Cerutti A *et al.* The apicoplast is important for the viability and persistence of *Toxoplasma gondii* bradyzoites. *Proc Natl Acad Sci USA* 2023;**120**:e2309043120.

Seeber F, Dubremetz JF, Boothroyd JC. Analysis of *Toxoplasma gondii* stably transfected with a transmembrane variant of its major surface protein, SAG1. *J Cell Sci* 1998;**111**:23–9.

Sindikubwabo F, Ding S, Hussain T *et al.* Modifications at K31 on the lateral surface of histone H4 contribute to genome structure and expression in apicomplexan parasites. *eLife* 2017;**6**:e29391.

Steentoft C, Vakhrushev SY, Joshi HJ *et al.* Precision mapping of the human O-GalNAc glycoproteome through SimpleCell technology. *EMBO J* 2013;**32**:1478–88.

Striepen B, Soldati D. Chapter 15–Genetic manipulation of *Toxoplasma gondii*. In: Weiss LM, Kim K (eds), *Toxoplasma gondii*(2nd edn), London, Academic Press, 2007, 391–418.

Teufel F, Almagro Armenteros JJ, Johansen AR *et al.* SignalP 6.0 predicts all five types of signal peptides using protein language models. *Nat Biotechnol* 2022;**40**:1023–5.

Tyanova S, Temu T, Sinitcyn P *et al.* The Perseus computational platform for comprehensive analysis of (prote)omics data. *Nat Methods* 2016;**13**:731–40.

Wadman M. Closure of U.S. *Toxoplasma* lab draws ire. *Science* 2019;**364**:109.

Wang D, Liu D, Yuchi J *et al.* MusiteDeep: a deep-learning based webserver for protein post-translational modification site prediction and visualization. *Nucleic Acids Res* 2020;**48**:W140–W6.

Warschkau D, Seeber F. Advances towards the complete *in vitro* life cycle of *Toxoplasma gondii*. *Fac Rev* 2023;**12**:1.

Waterhouse AM, Procter JB, Martin DM *et al.* Jalview Version 2–a multiple sequence alignment editor and analysis workbench. *Bioinformatics* 2009;**25**:1189–91.

Yu F, Haynes SE, Teo GC *et al.* Fast quantitative analysis of timsTOF PASEF data with MSFragger and IonQuant. *Mol Cell Proteomics* 2020;**19**:1575–85.

Zhou C-X, Zhu X-Q, Elsheikha HM *et al.* Global iTRAQ-based proteomic profiling of *Toxoplasma gondii* oocysts during sporulation. *J Proteomics* 2016;**148**:12–9.

Zhou DH, Wang ZX, Zhou CX *et al.* Comparative proteomic analysis of virulent and avirulent strains of *Toxoplasma gondii* reveals strain-specific patterns. *Oncotarget* 2017;**8**:80481–91.

Received 6 September 2024; **revised** 26 November 2024; **accepted** 19 December 2024